Journal of ELECTRONIC MATERIALS, Vol. 50, No. 3, 2021
https://doi.org/10.1007/s11664-020-08667-w

ORIGINAL RESEARCH ARTICLE

Optical Properties of Ternary Alloyed $CdSe_{1-x}Te_x$ Quantum Dots

NGUYEN THI THUC HIEN,[1,6] LE XUAN HUNG,[2] PHAM THU NGA,[1,3] and NGUYEN NHU DAT[1,4,5,7]

1.—Institute of Theoretical and Applied Research, Duy Tan University, 1 Phung Chi Kien, Hanoi 100000, Vietnam. 2.—Institute of Research and Development, Duy Tan University, 3 Quang Trung, Da Nang 550000, Vietnam. 3.—Institute of Materials Science, Vietnam Academy of Science and Technology, 18 Hoang Quoc Viet, Hanoi 100000, Vietnam. 4.—Faculty of Natural Sciences, Duy Tan University, 3 Quang Trung, Da Nang 550000, Vietnam. 5.—Institute of Physics, Vietnam Academy of Science and Technology, 10 Dao Tan, Hanoi 100000, Vietnam. 6.—e-mail: hien49@gmail.com. 7.—e-mail: nguyennhudat@duytan.edu.vn

Raman, absorption and photoluminescence (PL) spectra of ternary alloyed $CdSe_{1-x}Te_x$ quantum dots (QDs) with various values of x have been studied at room temperature. The average diameter of QDs is about 5.1 nm. The actual chemical composition was estimated by Raman spectroscopy. The values of 1.13 ± 0.06 eV and 1.01 ± 0.03 eV for the band gap bowing coefficient were obtained by fitting the composition dependence of the band gap and the PL peak energy, respectively, to the nonlinear Vegard formula. The PL quantum yields (QYs) were in the range of 24–53%. The relationship between PL peak wavelengths and quantum yields was investigated. It is shown that the QY dependence on the composition is associated with the crystalline quality of the alloy.

Key words: Ternary alloyed quantum dots, Raman, photoluminescence, optical band gap bowing, quantum yield, crystallinity

INTRODUCTION

Ternary alloyed $CdSe_{1-x}Te_x$ quantum dots (QDs) have attracted great attention for their advantages over their CdSe and CdTe binary base compounds regarding applications in photovoltaic devices, QD sensitized solar cells, biosensing and bioimaging instruments.[1–4] One of these advantages is the ability to tune the optical properties of the materials by controlling and altering the chemical composition without changing the QD size.[5] For certain values of composition x, the absorption and emission range of $CdSe_{1-x}Te_x$ QDs can be extended to the region of longer wavelengths than that of CdSe and CdTe QDs of the same size, i.e., the band structure parameters of such alloys are dependent on composition x. Thus, in addition to the size quantization effect, the component control provides an additional tool for adjusting the physicochemical properties of alloys. Therefore, the knowledge of the chemical composition is important when interpreting material properties that are composition-dependent. Normally, when making an alloy, it is common to estimate the chemical composition according to the composition of the starting precursors. However, the actual composition obtained in a fabricated material is not always the same as the initially selected ingredient, so it is necessary to determine the actual composition.

For determining the chemical composition of an alloy there are several methods such as Raman spectroscopy,[6,7] X-ray diffraction (XRD),[8,9] and X-ray photoelectron spectroscopy (XPS).[10,11] Energy-dispersive X-ray spectroscopy (EDX) is also used to determine element composition.[12] The method based on Raman measurements is shown to be fast and efficient with sufficient accuracy.[7] It is

(Received October 24, 2020; accepted December 2, 2020; published online January 4, 2021)

particularly useful to estimate the composition of nanocrystals of small size.

It was established that, at constant temperature, the lattice parameter and the composition of isostructural, isovalent semiconductor alloys obey approximately the known empirical Vegard's rule,[13] which states the linear relationship between these two quantities

$$a(x) = (1-x)a(\text{ AB}) + xa(\text{ AC})\ . \qquad (1)$$

Here $a(\text{ AB})$, $a(\text{ AC})$ and $a(x)$ denote the lattice constants of A-based compounds AB, AC and their mixed alloy $AB_{1-x}C_x$, respectively. It was also found that some physical properties of the alloys vary nonlinearly with composition. The nonlinear changing of the band gap with the component x is called "optical band gap bowing". The bowing formula for the band gap $E_g(x)$ of the bulk random alloy $CdSe_{1-x}Te_x$ has the form of a modified Vegard's formula[14,15]

$$E_g(x) = (1-x)E_g(\text{ CdSe}) + xE_g(\text{ CdTe}) - bx(1-x)\ , \qquad (2)$$

where b is the optical bowing coefficient defining the extent of nonlinearity in the variation of the band gap with the composition. $E_g(\text{ CdSe})$ and $E_g(\text{ CdTe})$ are the band gap of the binary bulk constituents. From Eq. 2 the bowing parameter b of the alloy is given by

$$b = \frac{E_g(x) - (1-x)E_g(\text{CdSe}) - \text{xE}_\text{g}(\text{CdTe})}{x(1-x)}. \qquad (3)$$

A theoretical model from first principles using the density-functional formalism was proposed by Zunger et al. in,[14,16] according to which the mismatch in the size and the chemical electronegativity of the alloying atoms, and the different lattice constants of the constituent structures result in the observed optical bowing. Based on this theory, the nonlinear effect for bulk alloy materials was successfully predicted and explained.

The quadratic relationship (2) is operative in some classes of semiconductor alloys and the bowing coefficient b, being positive or negative,[17] is almost constant with respect to composition x.[14] However, for alloys with large difference in the size and chemical properties of the atoms, for example, for CdS_xTe_{1-x}, the bowing coefficient may depend strongly on alloy composition.[14,18,19]

For nanocrystals, Bailey and Nie [5] have experimentally found the nonlinear relationship between the absorption/emission energies and the composition of alloyed CdSeTe QDs. They claimed that the observed nonlinear dependence is not solely caused by quantum size effect, although quantum confinement could play a certain role, and believed the mechanisms of optical bowing suggested by Zunger and co-workers are effective for nanoscopic alloys as well.

A number of theoretical and experimental studies on the optical bowing effect in alloyed ternary II-VI semiconductor QDs have been reported.[20–28] Gurusinghe and co-workers measured emission energies of CdS_xTe_{1-x} alloy QDs and revealed a strong nonlinearity in the dependence of the band gap on the S molar fraction.[21] Another alloyed ternary QD of II-VI group, CdS_xSe_{1-x} QDs, have been thoroughly studied.[22–25] The variation of the band gap of CdS_xSe_{1-x} QDs with size and composition has been experimentally studied by Swafford et al.[22] Applying the Vegard's relation, Eq. 2, they found that the bowing constant is actually the same for all QD sizes over the range of the experiment and is of the value similar to the bulk one. The composition nonlinear dependence of the band gap in CdS_xSe_{1-x} alloy QDs is also supported by the work of Ingole and co-workers[23] who studied the optical bowing effect both experimentally and theoretically. Tatikondewar and Kshirsagar performed theoretical calculations based on the density functional theory to investigate band-gap bowing in alloyed CdS_xSe_{1-x} QDs.[24] Plotting the variation in energy gap as a function of the sulfur composition, they showed that the curves for QDs of different diameters had almost the same curvature. This fact reflects that the bowing constant is weakly dependent on the size of QDs. Furthermore, the energy gap bowing in QDs is slightly stronger than in the bulk. In contrast, the optical measurements reported in[25] show that the optical band gap of $CdSe_xS_{1-x}$ QDs changes almost linearly with the Se concentration. Ternary alloy QDs of binary compounds CdSe and CdTe have also been studied with regard to composition-dependent optical properties.[26–28] The results of these investigations showed that the composition dependence of the optical band gap in alloyed CdSeTe QDs follows the quadratic polynomial form of Eq. 2, but the magnitude of the bowing constant is different among these works and in relation to its magnitude for bulk alloys reported in the literature. Therefore, further studies of the bowing effect in alloyed CdSeTe QDs are needed to make clearer whether the dependence of the band gap on composition in these QDs follows the nonlinear law and how the band gap bowing in QDs compares with that in the bulk.

In this paper, we present Raman scattering method for determining the chemical composition of alloyed $CdSe_{1-x}Te_x$ QDs. Using absorption and photoluminescence (PL) spectra we study the optical bowing effect and estimate the bowing constant of these QDs. We also determine the quantum yields (QYs) of the alloyed $CdSe_{1-x}Te_x$ QDs and try to explain the tendency of QY changing with the Te composition. Photoluminescence QY is a physical parameter used to evaluate the quality of the fluorophore. For applications, QDs should have high QYs.

EXPERIMENT

The procedure for preparing ternary alloyed $CdSe_{1-x}Te_x$ QDs has been described in detail in our previous papers.[29–31] Here we will give only a brief description of the fabrication. The sources of Cd, Se and Te were provided by reagents: acetate dehydrate (Cd $(Ac)_2.2H_2O$), selenium powder, and tellurium powder, respectively. Oleic acid (OA) was used as surface ligand and 1-octadecence(ODE) and triotylphosphine (TOP) as the reaction medium. The best conditions for the QD synthesis were found after careful investigation: the growth temperature is 260^0C, and the growth time is 10 min.

CHARACTERIZATION

The Raman scattering measurement was performed at room temperature on a XploRA-Horiba micro-Raman spectrometer. Light of 532-nm wavelength from a solid state laser was used for excitation. The incident laser light was focused on the sample to a spot of 1 μm in diameter. The spectral resolution was 2 cm^{-1}. The acquisition time ranged from 30 s to 120 s, but normally was 30 s. A charge coupled device (CCD) with four gratings with 600 slits/mm, 1200 slits/mm, 1800 slits/mm and 2400 slits/mm was used to detect scattered light from the sample. The measuring range was from 100 cm^{-1} to 4000 cm^{-1}.

Transmission electron microscopy (TEM) measurements were carried out using a JEOL Jem 1010 microscope operating at 100 kV. The TEM images of the CdTeSe QD samples have been presented in Ref. 30. The average QD size of 5.1 nm was determined from the obtained TEM images. The alloy structure was analyzed by powder X-ray diffraction (XRD) patterns. For all samples, the crystal lattice was found to be a zinc-blende structure.

The ultraviolet-visible (UV-Vis) absorption spectra were measured within the wavelength range of 200–1000 nm using a Shimadzu (UV-1800) UV-Vis spectrophotometer. The PL spectra were measured using a Fluorolog-322 system (Jobin-Yvon), the excitation at 532 nm was provided by a Xenon 450 W lamp. The detector is a photomultiplier, measuring range from 250 nm to1000 nm. All PL spectra were measured under the same conditions. The solution concentrations were adjusted in order to all present an optical density of 0.03 at 532 nm so that the emission intensities of the different samples can be compared (although affected by the measurement system spectral response). For QY measurement we excited the sample as well as the known dye (Rhodamine 101) in ethanol as reference (QY = 96%) with the 532-nm light.

RESULTS AND DISCUSSION

Chemical Composition Determination

We have determined the chemical composition of alloyed $CdSe_{1-x}Te_x$ QDs by using Raman spectra, and compared it with the initial precursor concentration. The Raman spectra of the QDs measured at room temperature are presented in Fig. 1. It is seen that the first-order Raman spectra exhibit a two-mode behavior with CdTe-like (LO1) (about 159 cm^{-1}) and CdSe-like (LO2) (about 189 cm^{-1}) longitudinal optical phonon peaks.[32] The second-order peak is situated at higher frequency. Because of non-resonant Raman regime, in the second-order we can observe only one broad peak of combination mode (LO1+LO2) at about 350 cm^{-1}. The first-order longitudinal optical phonon frequencies (CdTe-like and CdSe-like) are used to determine the alloy composition because they change with the composition. The peak intensity of the phonon modes also change with composition x. As seen from Fig. 1, when x increases, the CdSe-like mode peak shifts toward the CdTe-like one, and both coincide with the LO phonon frequency of CdTe at $x = 1$. At the same time, the peak intensity of CdTe-like mode increases and, conversely, the intensity of CdSe-like mode decreases.

To determine the chemical composition of alloyed CdSeTe QDs using Raman spectra, it is assumed that the change of the Raman frequency with composition is the same for the bulk and QD samples.[6] Comparing the Raman optical-mode peak positions for QDs with those of the bulk of the same composition, we can assess the composition of the alloyed QDs. In principle, we can use either phonon frequencies of CdTe-like mode (ω_{LO1}) or CdSe-like mode (ω_{LO2}) of $CdSe_{1-x}Te_x$ QDs. However, the phonon frequencies in nanocrystals are affected by phonon confinement and other effects (e.g., strain from the medium surrounding nanocrystals).[7,33,34] The phonon confinement may cause a redshift of the Raman peak frequency, whereas the shift due to strain is opposite, so an error exists when determining the composition by using only one phonon mode. Since both LO1 and LO2 modes are affected by these effects in a similar way; the error can be limited if we use the frequency difference of the LO1 and LO2 phonons.[6] Figure 2 presents the difference

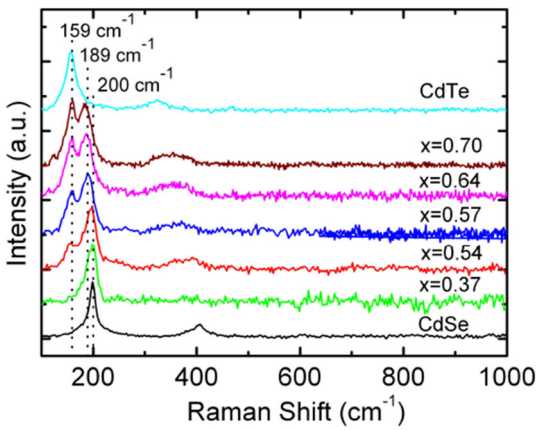

Fig. 1. Raman spectra of ternary alloyed $CdSe_{1-x}Te_x$ measured at room temperature. The excitation wavelength is 532 nm.

between the LO1 and LO2 phonon frequencies as a function of composition for our QDs and for the bulk $CdSe_{1-x}Te_x$ sample.[35]

The composition x of alloyed CdSeTe QDs estimated as starting precursors ratio and the corresponding composition determined by Raman spectra are presented in Table I. Raman spectra are used to determine the composition of CdS_xSe_{1-x} nanocrystals; the authors of Ref. 6 achieved an accuracy as high as $\Delta x = \pm 0.03$. In our case, the accuracy is lower, $\Delta x = \pm 0.05$, especially for the compositions close to the base binary compounds CdSe and CdTe. At these values of composition, the CdTe-like and CdSe-like bands are less separated or the intensity of one band becomes weaker, and then it is difficult to determine accurately the peak position of the band. As seen from Table I, the amount of Te present in the alloys is larger than its estimate from initial precursors ratio (nominal composition). It may be because Te reacts much faster with Cd relative to Se.[5]

We have also determined the chemical composition by X-ray diffraction (not shown here). The results are similar to that determined by Raman spectra. Therefore, we can say the Raman technique is suitable for determining composition of alloyed QDs. For these QDs with two-LO-phonon-mode behavior, the accuracy of this technique is high for compositions at which the two modes are clearly distinguished.

Bowing Effect

The absorption spectra of the alloyed $CdSe_{1-x}Te_x$ QDs measured at room temperature are shown in Fig. 3. As seen from the figure, the slope of absorption curves varies with the Te composition in the QDs. The intercept of the slope and the wavelength axis represents the absorption onset whose composition dependence also describes the same dependence of the optical band gap of the sample. Therefore, we will denote the absorption onset as the band gap E_g. Depending on the value of x, the absorption onset can range from 650 nm to 800 nm: with increasing x, the absorption onset moves from 646 nm (for CdSe, $x = 0$) to 800 nm (at $x = 0.57$) and then back down to 674 nm (for CdTe, $x = 1$). This means that the absorption of $CdSe_{1-x}Te_x$ alloy QDs can be shifted to wavelengths longer than that of CdSe and CdTe, i.e. the optical band gap of ternary $CdSe_{1-x}Te_x$ QDs is smaller than the band gap of both CdTe and CdSe constituents. This fact is reflected in Fig. 4. The composition dependence of the band gap of bulk alloyed $CdSe_{1-x}Te_x$ is also plotted for comparison. The optical bowing effect is clearly shown in the plots. A similar shape of the composition band gap curve is also found in Refs. 5,14,19,26,36,37. A minimal E_g is observed for our QDs at $x \approx 0.5$, different from $x \approx 0.4$ in Refs. 36,37 for bulk alloy, $x \approx 0.6$ (for both QDs and the bulk) in Ref. 5. This value of x for QDs is consistent with that estimated in Ref. 26 where the minimum in E_g is found at $x \approx 0.5$ for both QDs and bulk alloys. In contrast, although Han et al.[28] confirmed the nonlinear dependence of the band gap energy on the composition in QDs, they revealed a gradual decrease of the band gap with increasing Te composition in $CdSe_{1-x}Te_x$ QDs from CdSe ($x = 0$) to CdTe ($x = 1$), i.e., the minimal E_g is in CdTe QDs.

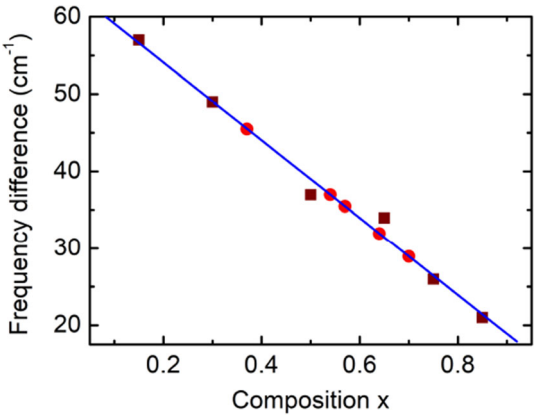

Fig. 2. The difference of CdSe-like (ω_{LO2}) and CdTe-like (ω_{LO1}) LO mode frequencies versus composition x for $CdSe_{1-x}Te_x$ QDs (solid circles) and the bulk sample (solid squares). The solid line is the linear fit to the bulk data taken from[35].

There are various values of the bowing parameter b for $CdSe_{1-x}Te_x$ alloys reported in the literature. The bowing curves obtained from absorption experiment are described by the coefficient b of 0.8 eV,[37] 0.94 eV[38] for bulk samples, and 0.59 eV,[39] 2.07 eV[40] for thin films. Theoretical calculation provides a value of 0.75 eV for b in bulk CdSeTe alloys.[14] As regards alloyed $CdSe_{1-x}Te_x$ QDs, the measured bowing coefficient $b = 0.50$ eV was reported in Ref. 28. This value is smaller than the bulk one. Fitting our absorption data by formula (2) (Fig. 4), the best fit value for the bowing coefficient is $b = (1.13 \pm 0.06)$ eV. We obtained also the fitting value $b = (1.06 \pm 0.01)$ eV for bulk data extracted from Ref. 5. Our results showed that, in contrast to the results of Ref. 28, the bowing effect in CdSeTe alloyed QDs is somewhat stronger (with greater b) than in the bulk. This means the composition may have greater influence on nanocrystals than on the bulk.

Figure 5 displays photoluminescence (PL) spectra measured at room temperature for alloyed $CdSe_{1-x}Te_x$ QDs with various values of Te composition. All PL spectra exhibit a clear band-edge emission peak with full width at half-maximum (FWHM) of about 80 nm. This means the alloyed $CdSe_{1-x}Te_x$ QDs are pure and have a large size distribution (with an average diameter of 5.1 nm).The PL peak energy in dependence on Te composition is presented in Fig. 6 for $CdSe_{1-x}Te_x$ QDs. Since the PL peak energy defines the band gap E_g of the sample, it can be seen from this figure the variation of the band gap of alloyed QDs with tellurium content. The E_g data from PL

Table I. $CdSe_{1-x}Te_x$ alloy QDs composition determined from initial precursors ratio (nominal composition) and by Raman spectra (actual composition).

Nominal composition	Difference $(\omega_{LO2} - \omega_{LO1})$ (cm^{-1})	Actual composition
0.2	45.46	0.37
0.4	36.89	0.54
0.5	35.51	0.57
0.6	31.97	0.64
0.8	28.95	0.70

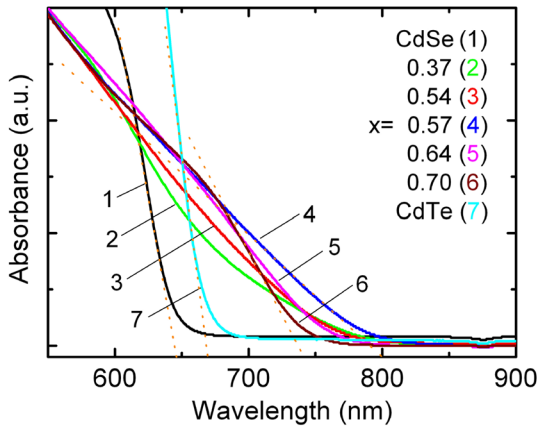

Fig. 3. Absorption spectra of $CdSe_{1-x}Te_x$ QDs with different composition x.

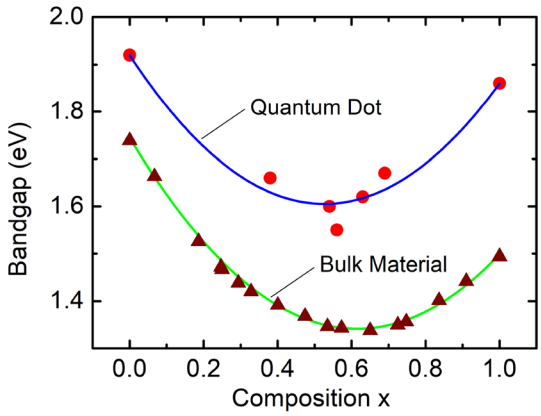

Fig. 4. $CdSe_{1-x}Te_x$ band gap E_g as a function of Te composition, solid circles for QDs and solid triangles for the bulk (extracted from Ref. 5). Solid lines are the fits using formula (2).

measurements for alloyed $CdSe_{1-x}Te_x$ QDs reported in Ref. 27 are also included in the figure for comparison. It is seen again that the minimal PL peak energy of our samples is observed for Te composition $x \approx 0.5$. This value is consistent with that in absorption onsets and smaller than that in Refs. 27, 36, 41.

The fits to experimental E_g data using Eq. 2 are displayed in Fig. 6 as solid lines. The fitting bowing constant for our samples is $b = (1.01 \pm 0.03)$ eV. This value of b is smaller than our value 1.13 eV obtained from absorption spectra reported above.

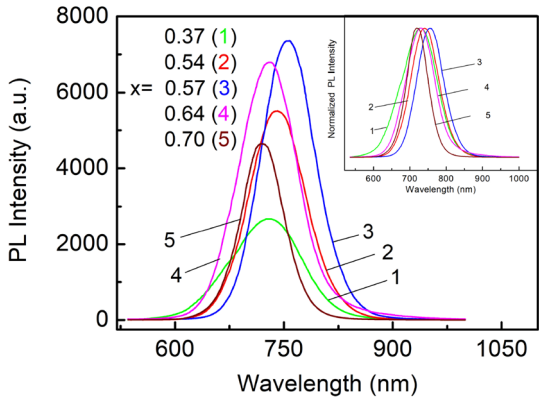

Fig. 5. PL spectra of $CdSe_{1-x}Te_x$ QDs with different composition x measured at room temperature. The excitation wavelength is 532 nm. In the inset are the normalized spectra.

Fitting the data from Ref. 27 provides a value of 1.33 eV for the bowing constant, which is greater than our value of 1.01 eV. Our bowing constant for QDs is slightly greater than the 0.97 eV value estimated from PL spectra of CdSeTe films in Ref. 42, the experimental value 0.78 eV[27] and the theoretical 0.904 eV[41] for the bulk counterparts. The large values of the bowing parameter obtained from PL spectra in alloyed QDs compared with bulk alloys once again support the conclusion of the more significant influence of composition in the nanocrystals mentioned above. It should be noted that the authors of Ref. 24 also found that the bowing coefficients in bulk samples were smaller than in CdS_xSe_{1-x} QDs of different sizes.

Since the band-edge peaks in PL spectra are quite clear, the peak positions can be well determined. Consequently, the band gap energies determined from PL spectroscopy for alloyed QDs with different composition are more accurate than in the absorption case in the present study, resulting in better bowing coefficient in value.

Quantum Yield

We have measured relative PL quantum yields (PL QYs) of alloyed $CdSe_{1-x}Te_x$ QDs. The results are displayed in Table II. As seen in the table, as x increases from 0.37 to 0.57, the emission peak position increases from 731 nm to 756 nm and QY increases from 24.9% to 52.6%. As x continues to increase from 0.64 to 0.70, the peak position

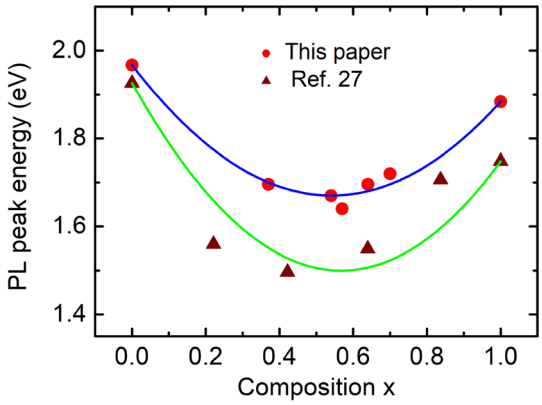

Fig. 6. PL peak energy as a function of Te mole fraction x of $CdSe_{1-x}Te_x$ QDs. For comparison, the data from Ref. 27 are marked as solid triangles. Solid lines are the fits using formula (2).

Table II. The PL peak position and quantum yield of alloyed $CdSe_{1-x}Te_x$ QDs measured at room temperature.

x	PL Peak position (nm)	PL QY(%)
0	630	
0.37	731	24.9
0.54	742	41.0
0.57	756	52.6
0.64	731	53.4
0.70	720	27.1
1.00	658	

decreases from 731 nm to 720 nm and QY decreases from 53.4% to 27.1% as well. Figure 7 shows the dependence of PL peak wavelength and QY on Te composition x where the solid lines are just a guide to the eye. It can be said that the emission wavelengths and QY follow almost the same trend in composition dependence.

It is thought that a relationship between QY of alloyed $CdSe_{1-x}Te_x$ QDs and their crystallinity may provide a possible explanation for the change of QY with composition. According to Wei et al.,[14] $CdSe_{1-x}Te_x$ alloy has a bowing coefficient larger than the band gap difference of the binary constituents (1.72 eV for CdSe and 1.48 eV for CdTe at 300 K). A minimal band gap E_g occurs at a Te content of $x<1$. At low Se content, i.e. $x \leq 1$; therefore, adding Se into CdTe reduces the band gap of the alloy (the right half of the bowing curve in Figs. 4, 6). The FWHM of the PL spectra, in this case, increases and the QY also increases. Further increase of Se content, i.e., decreasing the Te content from $x = 0.6$ to $x = 0.37$, leads to an increase of the band gap (the left half of curves in Figs. 4, 6), but at the same time, this makes the quality of the alloy worse due to the large miscibility gap and the poor p-type dupability of CdSe. A decrease in the quality of the alloy means, among others, a decrease

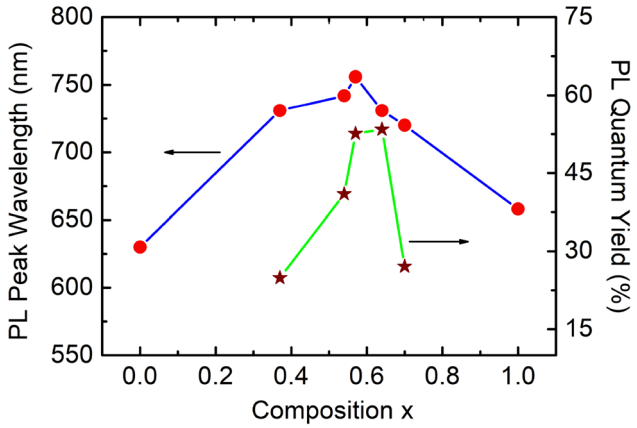

Fig. 7. PL peak wavelength (solid circles) and PL QY (asterisks) for $CdSe_{1-x}Te_x$ alloyed QDs as a function of Te mole fraction (x). The solid lines are for a guide to the eyes.

in the crystallinity of the alloy. This is reflected in the reduction in the strength ratio between the second-order LO Raman peaks and the fundamental one, since the strength and sharpness of the high-order phonon peaks are generally sensitive to the degree of the crystalline perfection.[43] From Raman data of $CdSe_{1-x}Te_x$ alloy QDs (Fig. 1) we obtained the change of the intensity ratio with composition as follows. As x decreases from 0.70 to 0.64 (Se content increases from 0.30 to 0.36), the ratio increases from 0.26 to 0.29, that means the crystallinity (and the quality) of the QDs increases. For $x = 0.57, 0.54, 0.37$ the ratio decreases gradually and has values 0.41, 0.3 and 0.08, respectively, indicating the decrease of the crystallinity and the quality as well. Reducing the quality of the alloy QDs leads to a decrease of their QY (see Fig. 7). It should be noted that for alloyed CdSeTe QDs we can find the same trend in Se composition dependence of the second-order Raman peaks in Ref. 43, and of the quantum yields in Refs. 44,45.

CONCLUSION

In summary, we have studied the Raman spectra, absorption and photoluminescence properties of ternary alloyed $CdSe_{1-x}Te_x$ QDs ($x = 0, 0.37, 0.54, 0.57, 0.7, 1$) at room temperature. The chemical composition was estimated using Raman spectroscopy. The accuracy of the estimation is of $\Delta x = \pm 0.05$ but worse for small x. The bowing coefficient has been determined by fitting the composition dependence of the band gap and PL peak position energy to the nonlinear Vegard formula. The better value of the bowing coefficient is (1.01 ± 0.03) eV obtained from PL peak position analysis. This value for alloy CdSeTe QDs is greater than that for the bulk counterpart, indicating a more significant influence of chemical composition on nanocrystals than on the bulk. The PL peak positions, PL FWHM and QYs of QDs are related each other. The highest QY is 53.4% achieved at

$x = 0.64$ and the lowest is 24.9% at $x = 0.37$ over the composition range of the experiment. Quantum yields and PL peak wavelengths have a similar trend in composition dependence. This behavior may be related to the alloy's quality (the crystallinity) dependence on the composition. This leads to suggestion that there might be a close relation between the alloyed QDs QY and the alloy quality in general, and the alloy's crystallinity in particular: the better the alloy crystallinity the higher QY. To the best of our knowledge, there are no reports on the connection of alloy QY with its crystallinity and composition in existing literature. Therefore, these results might be of certain significance in the preparation and application in photovoltaic devices.

ACKNOWLEDGEMENTS

The authors would like to thank anonymous reviewers for their valuable comments and suggestions. This research is funded by the Vietnam National Foundation for Science and Technology Development (NAFOSTED) under Grant No. 103.03-2018.03. The authors also thank the National Key Laboratory for Electronic Materials and Devices (IMS) and Duy Tan University for giving facilities to carry out the research.

CONFLICT OF INTEREST

The authors declare that they have no known competing financial interests or personal relationships that could have appeared to influence the work reported in this paper.

REFERENCES

1. H. Zou, M. Liu, D. Zhou, X. Zhang, Y. Liu, B. Yang, and H. Zhang, J. Phys. Chem. 121, 5313 (2017).
2. R. Soltani, A.A. Katbab, K. Schaumberger, N. Gasparini, Ch. J. Brabec, S. Rechberger, E. Spiecker, A.G. Alabau, A. Ruland, A. Saha, D. M. Guldi, V. Sgobba, and T. Am, J. Mater. Chem. C 5, 654 (2017).
3. Zh. Han, L. Chen, Q. Weng, Y. Zhou, L. Wang, Ch. Li, and J. Chen, Sens. Actuators B 258, 508 (2018).
4. B. Xing, W. Li, X. Wang, H. Dou, L. Wang, K. Sun, X. He, J. Han, H. Xiao, J. Miao, and Y. Li, J. Mater. Chem. 20, 5664 (2010).
5. R.E. Bailey and Sh. Nie, J. Am. Chem. Soc. 125, 7100 (2003).
6. A. Tu and P. D. Persans, Appl. Phys. Lett. 58, 1506 (1991).
7. Yu. M. Azhniuk, Yu.I. Hutych, V.V. Lopushansky, L.A. Prots, A.V. Gomonnai, and D.R.T. Zahn, Phys. Status Solidi (c) 6, 2064 (2009).
8. A.P. Stuckes and G. Farrell, J. Phys. Chem. Solids 25, 477 (1964).
9. J. Litwin, Phys. Status Solidi 5, 551 (1964).
10. M.R. Uddin, S. Majety, J. Li, J.Y. Lin, and H.X. Jiang, J. Appl. Phys. 115, 093509 (2014).
11. I. Shtepluk, O. Khyzhun, G. Laskharev, V. Khomyak and V. Lazorenko, Acta Phys. Pol. A 122, 1034 (2012).
12. W. Jiang, A. Singhal, J. Zheng, Ch. Wang, and W.C.W. Chan, Chem. Mater. 18, 4845 (2006).
13. J.E. Bernard and A. Zunger, Phys. Rev. B 34, 5992 (1986).
14. S.-H. Wei, S.B. Zhang, and A. Zunger, J. Appl. Phys. 87, 1304 (2000).
15. L. Hannachi, N. Bouarissa, Superlattices Microstruct. 44, 794 (2008).
16. J.E. Bernard and A. Zunger, Phys. Rev. B 36, 3199 (1987).
17. S.A. Yamini, V. Patterson, and R. Santos, ACS Omega 2, 3417 (2017).
18. S.-H. Wei and A. Zunger, Phys. Rev. Lett. 76, 664 (1996).
19. L. Bellaiche, S.-H. Wei and A. Zunger, Phys. Rev. B 54, 17568 (1996).
20. S. Wageh, A. Al-Ghamdi, A. Jilani, and J. Iqba, Nanomaterials 8, 979 (2018).
21. N.P. Gurusinghe, N.N. Hewa-Kasakarage, and M. Zamkov, J. Phys. Chem. C 112, 12795 (2008).
22. L.A. Swafford, L.A. Weigand, M.J. Bowers, J.R. McBride, J.L. Rapaport, T.L.Watt, S.K. Dixit, L.C. Feldman and S.J. Rosenthal, J. Am. Chem. Soc. 128, 12299 (2006).
23. P.P. Ingole, G.B. Markad, D. Saraf, L. Tatikondewar, O. Nene, A. Kshirsagar, and S. K. Haram, J. Phys. Chem. C 117, 7376 (2013).
24. L. Tatikondewar and A. Kshirsagar, Phys. Chem. Chem. Phys. 19, 14495 (2017).
25. L.A. Thi, N.D. Cong, N.T. Dang and N.X. Nghia, and V.X. Quang, J. Electron. Mater. 45, 2621 (2016).
26. B. Hou, D. Parker, G.P. Kissling, J.A. Jones, D. Cherns, and D. J. Fermín, J. Phys. Chem. C 117, 6814 (2013).
27. J. Liu, W. Yang, Yu. Li, L. Fan, and Y. Li, Phys. Chem. Chem. Phys. **16**, 4778 (2014).
28. Zh. Han, L. Ren, L. Chen, M. Luo, H. Pan, Ch. Li, J. Chen, J. Alloys Compd. 699, 216 (2017).
29. L.X. Hung, P.N. Thang, H.V. Nong, N.H. Yen, V.D. Chinh, L.V. Vu, N.T.T. Hien, W.D. de Marcillac, P.N. Hong, N.T. Loan, C. Schwob, A. Maître, N.Q. Liem, P. Bénalloul, L. Coolen, and P.T. Nga, J. Electron. Mater. 45, 4425 (2016).
30. L.X. Hung, P.D. Bassène, P.N. Thang, N.T. Loan, W.D. de Marcillac, A.R. Dhawan, F. Feng, J.U. Esparza-Villa, N.T.T. Hien, N.Q. Liem, L. Coolen, and P. T. Nga, RSC Adv. 7, 47966 (2017).
31. L.X. Hung, P.T. Nga, N.N. Dat, and N.T.T. Hien, J. Electron. Mater. 49, 2568 (2020).
32. A.V. Bragas, C. Aku-Leh, S. Costantino, A. Ingale, J. Zhao, and R. Merlin, Phys. Rev. B 69, 205306 (2004).
33. G. Scamarcio, M. Lugara, and D. Manno, Phys. Rev. B 45, 13792 (1992).
34. A. Roy and A.K. Sood, Phys. Rev. B 53, 12127 (1996).
35. M. Gorska and W. Nazarezicz, Phys. Status Solidi (b) **65**, 193 (1974).
36. H.C. Poon, Z.C. Feng, Y.P. Feng, and M.F. Li, J. Phys.: Condens. Matter 7, 2783 (1995).
37. M.S. Brodin, N.I. Vitrikhovskii, A.A. Kipen, and I.B. Mizetskaya, Fiz. Tekh. Poluprovodn. 6, 601 (1972).
38. L.V. Prythina, V.V. Volkov, A.N. Mentser, A.V. Vanyukov, and P.S. Kireev, Fiz. Tekh. Poluprovodn. 2, 611 (1968).
39. R. Islam, H.D. Banerjee, D.R. Rao, Thin Solid Films 266, 215 (1995).
40. P.D. More, G.S. Shahane, L.P. Deshmukh, and P.N. Bhosale, Mater. Chem. Phys. 80, 48 (2003).
41. N. Tit, I.M. Obaidat, and H. Alawadhi, J. Phys.: Condens. Matter 21, 075802 (2009).
42. E.M. Campo, Th. Hierl, J.C.M. Hwang, Y. Chen, G. Brill, and N.K. Dhar, Proc. SPIE 5564, 86 (2004).
43. Z.C. Feng, P. Becla, L.S. Kim, S. Perkowitz, Y.P. Feng, H.C. Poon, K.P. Williams, and G.D. Pitt, J. Cryst. Growth 138, 239 (1994).
44. L. Song, J. Duan, and J. Zhan, Mater. Lett. 64, 1843 (2010).
45. G.-X. Liang, M.-M. Gu, J.-R. Zhang, and J.-J. Zhu, Nanotechnology 20, 415103 (2009).